

INJECTION AND EXTRACTION BEAM TRANSPORT SYSTEM FOR THE HIMAC SYNCHROTRON

K. Noda, M. Kanazawa, A. Itano, M. Kumada, K. Sato, M. Sudou, E. Takada, T. Kohono, A. Kitagawa, H. Ogawa, Y. Sato, S. Yamada, T. Yamada and Y. Hirao
National Institute of Radiological Sciences, Anagawa, Chiba-shi, Chiba 260, Japan

K. Endo
National Laboratory for High Energy Physics KEK, Oho, Tsukuba-shi, Ibaraki 305, Japan

T. Chugun, K. Katsuki, T. Morii and N. Suetake
Toshiba Corp., Uchisaiwai-cho, Tokyo 100, Japan

Abstract

The Heavy Ion Medical Accelerator in Chiba (HIMAC) will be the first heavy ion synchrotron complex for the clinical treatment of tumor in Japan. This paper describes the design of the injection and the extraction beam transport system for the HIMAC synchrotron and the results of the field measurements of the magnets in the injection line.

Introduction

The HIMAC is now under construction at National Institute of Radiological Sciences (NIRS)¹. In the HIMAC facility, especially, the injection beam transport system between the linac cascade and two synchrotron rings is required to transport the beam alternately to two rings in the same condition. The requirement is satisfied by using a fast switching magnet. In addition, the system is designed to transport a beam with a selected charge to mass ratio in the beam analyzing section and to adjust the beam to an injection condition at the entrance of each ring for an efficient multiturn injection. Furthermore, it is designed for the beam with the maximum magnetic rigidity of 1.42 T·m to be transported. This rigidity corresponds to the energy of 6 MeV/u for ions with a charge to mass ratio of 1/4.

The upper and the lower extraction beam transport systems are designed to transport a slowly extracted beam from each ring independently to each high-energy beam delivery system in the same condition because of an efficient radiation therapy. The layout of the injection and the extraction beam transport system are shown in Fig. 1.

Injection Beam Transport System

Design of the system

The injection beam transport system is designed to transport the beam with quality listed at Table 1 from the linac and to obtain a good efficiency of the beam transmission and to be adjustable the beam to the optical condition of the multiturn injection to the ring.

As shown in Fig. 1(a), this system consists of five bending magnets(BM), a switching magnet(SWM), thirty one quadrupole magnets(QM), seven horizontal and nine vertical steering magnets(ST), seven profile monitors(PRN), three Faraday cups(FCN) and a horizontal slit(SLT).

The basic requirements of the system are as follows.

- (1) Beam should be injected alternately to two rings in the same condition for a short time.
- (2) Beam should be transported with the smallest loss.
- (3) The Twiss parameters at the entrance of each ring should be easily adjustable to match the condition of the multiturn injection.
- (4) Beam of ion with different charge to mass ratio should be separated.
- (5) The momentum of the beam should be analyzed for an efficient beam transportation in the injection line and an easy beam tuning in the ring.

In order to realize the above conditions, the following scheme is adopted and designed.

A fast switching magnet (SWM) is designed for the

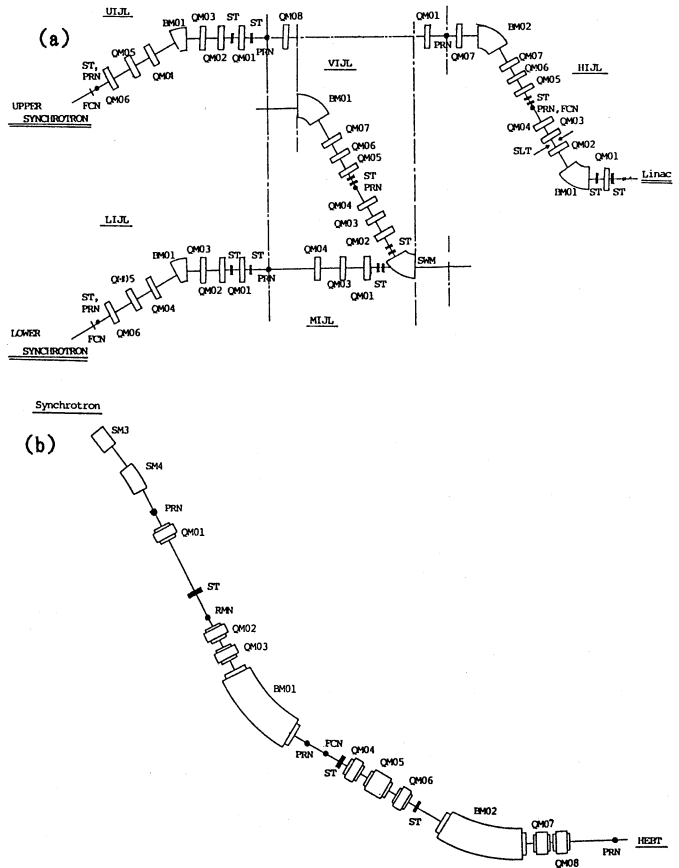


Fig.1 The layout of (a) the injection and (b) the extraction beam transport system.

alternating operation of two rings. The rising and the falling time of the power supply for SWM are 140 msec, respectively and the stability in the flat top with the time of about 10 msec is expected to be equal or less than $\pm 1 \times 10^{-4}$, which is confirmed by using dummy load.

To suppress the beam loss, a required size of beam duct is determined by considering a centroid displacement of the beam as well as an acceptance for the betatron oscillation and for the momentum spread. First, the beam optics is calculated by using the program MAGIC². The initial and the final condition of the injection beam transport system are listed at Table 1 and the beta and dispersion functions are shown in Fig. 2. Second, the position and the field strength of the steering magnets (ST) and the position of the beam profile monitors (PRN) are determined for the centroid displacement to be suppressed within the size of 10 mm which is caused by a misalignment and a field error of the magnets assumed at Table 2.

For easily beam tuning, in the HIJL and the VIJL section, a mirror symmetry optics is adopted to realize the waist to waist transportation with a doubly achromatic condition. In each section, the first quadrupole magnet (QM01) plays a role for decreasing the beam size in the

direction of the gap of the following bending magnet (BM01). The dispersion function and the derivative of the beta functions at the symmetry point are set to be zero by three quadrupole magnets (QM02~QM04). In the UIJL and the LIJL section, on the other hand, the injection beam is adjusted to the condition of the multiturn injection to each ring. Since a doubly achromatic condition at the entrance of each ring is realized by two quadrupole magnets (QM04, QM06), the electrostatic field at a gap between a septum and an electrode of the inflector can be reduced. Other four quadrupole magnets are prepared to match the beta function and its derivative at the entrance of the ring to the condition of the multiturn injection.

A beam momentum and a charge to mass ratio are analyzed by measuring the field strength of the first bending magnet (BM01) with a NMR and by using the horizontal slit (SLT) in the HIJL section and that in the last transport line of the linac. The measurement result is referred to the magnetic field strength of the main magnets corresponding to a flat base of an excitation pattern of the ring.

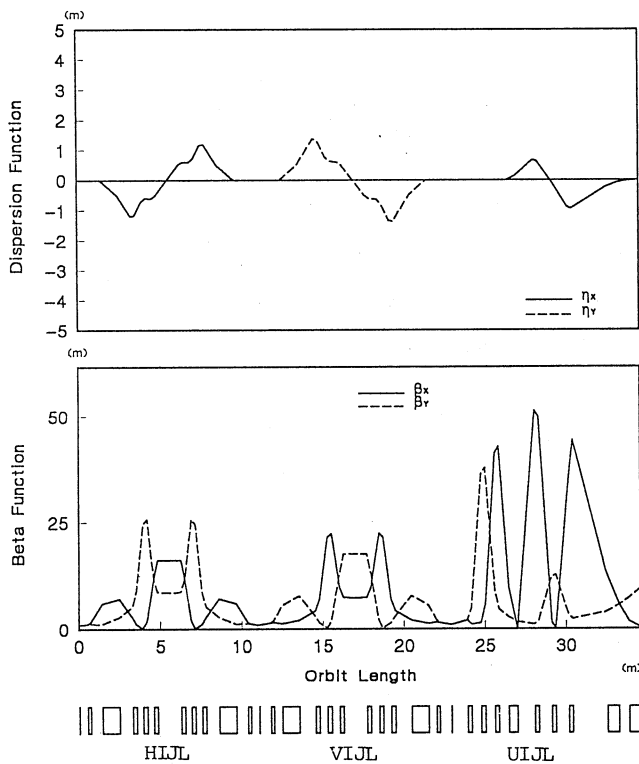


Fig. 2 Beta and dispersion functions in the injection line.

Table 1
Initial and final condition for the injection line

	initial condition	final condition
β_x	1.0 m	0.325 m
β_y	1.0 m	10.976 m
α_x	0	0
α_y	0	-2.05
η_x	0	0
η_y	0	0
ϵ_x	26.4 π mm·mrad *1	
ϵ_y	26.4 π mm·mrad	
$\Delta P/P$	$\pm 0.3\%$ *2	

*1 and *2 correspond an acceptance for the betatron oscillation and for the momentum spread, respectively.

Table 2

Assumed quantity of the misalignment and the field error

1. Bending magnet	
$\Delta X, \Delta Y$	± 0.3 mm
ΔS	± 0.5 mm
Rotation of X, Y and S axis	± 1.0 mrad
$\Delta BL/BL$	$\pm 1.5 \times 10^{-3}$
2. Quadrupole magnet	
$\Delta X, \Delta Y$	± 0.3 mm
ΔS	± 0.5 mm
Rotation of S axis	± 2.0 mrad
$\Delta GL/GL$	$\pm 4.0 \times 10^{-3}$
3. Centroid displacement of beam from linac	
$\Delta X, \Delta Y$	± 2.5 mm
$\Delta X', \Delta Y'$	± 2.5 mrad
4. Centroid displacement of beam from ring	
$\Delta X, \Delta Y$	$\pm 1.0, \pm 1.5$ mm
$\Delta X', \Delta Y'$	0, ± 0.5 mrad

Design and measurement of the magnets

The bending and quadrupole magnets in the injection beam transport system have been already designed and manufactured except for the SWM. The profile of the pole face of the magnets is designed so that the field uniformity distribution is equal or less than $\pm 5 \times 10^{-4}$ for the bending magnets and $\pm 1 \times 10^{-3}$ for the quadrupole magnets. Furthermore, the pole end of the magnets is cut not only to suppress the change of the effective length due to the change of field level but also to improve the uniformity of the distribution of the integrated field strength and gradient (BL and GL). The end cut of the bending and the quadrupole magnets are estimated according to Rogowski's method and the method presented in the ref. 3, respectively.

The magnetic field of the bending and the quadrupole magnets are measured by using a Hall Probe and a long twin coil, respectively⁴. Fig. 3 shows typical measured results on the field uniformity ($\Delta BL/BL$ and $\Delta GL/GL$) for the bending and quadrupole magnets. The uniformity was less than 5×10^{-4} for the bending magnets and 1×10^{-3} for the quadrupole magnets in the required region ($-25 \text{ mm} \leq X \leq 25 \text{ mm}$). The fringing field of the bending magnets is also measured. As the results of the measurements, K_1 values (quadrupole component)⁶ of the magnets without and with a field clump (HIJL-BM02) are estimated at 0.69 and 0.73, respectively. Considering the measured results, therefore, the parameters for the beam optics will be changed a little.

Extraction beam transport system

The extraction beam transport system in each ring consists of two 33° bending magnets, eight quadrupole magnets, three horizontal and vertical steering magnets (ST), three profile monitors (PRN) with a wide intensity range⁵, a ripple monitor (RMN) and the fast beam shutter (FCN) as shown in Fig. 1(b).

By the same manner as in the case of the injection beam transport system, the beam optics from the entrance of the first electrostatic deflector in the ring to that of the high energy beam delivery system is calculated and shown in the Fig. 4 and the steering magnets and the profile monitors are assigned at the line. The initial and the final condition for the beam optics is summarized at Table 3.

In addition, the fast beam shutter is installed not only to assure the accurate irradiation dose for the clinical treatment and the biological experiments but also for the beam from ring to be adjusted to the optimum condition for a beam profile, a beam centroid and a spill structure by using the profile monitors and the

ripple monitor and by tuning the beam extraction apparatuses in the ring before transportation to the high energy beam delivery system.

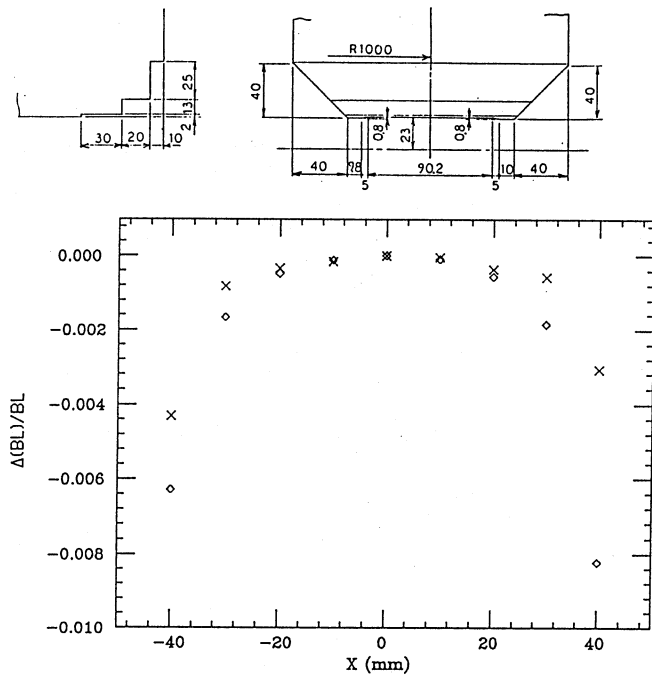


Fig. 3(a) Measured distribution of the uniformity ($\Delta BL/BL$) for HIJL-BM01 ($\rho=1.0\text{m}$, Gap=46mm, max.B=1.42T) X and \diamond indicate the distribution corresponding to B=0.71T and B=1.42T, respectively. The profile of the pole face is also shown (right; profile of pole, left; end cut).

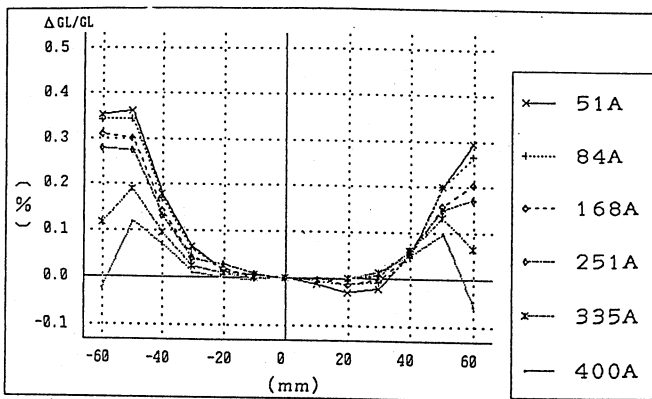
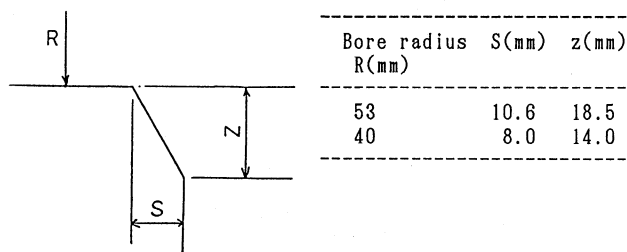


Fig. 3(b) Measured distribution of the uniformity ($\Delta GL/GL$) for MIJL-QM03 (bore radius=53mm, max.G= 6.4T/m) corresponding to various excitation current. The profile of the end cut is also shown.

Table 3
Initial and final condition for the extraction line

	initial condition	final condition
β_x	5.0 m	1.0 m
β_y	5.49m	1.0 m
α_x	0	0
α_y	-1.27	0
η_x	-0.5	0
η_y	0	0
ϵ_x	10.0 π mm·mrad *1	
ϵ_y	10.0 π mm·mrad	
$\Delta P/P$	$\pm 0.2\%$ *2	

*1 and *2 correspond an acceptance for the betatron oscillation and for the momentum spread, respectively.

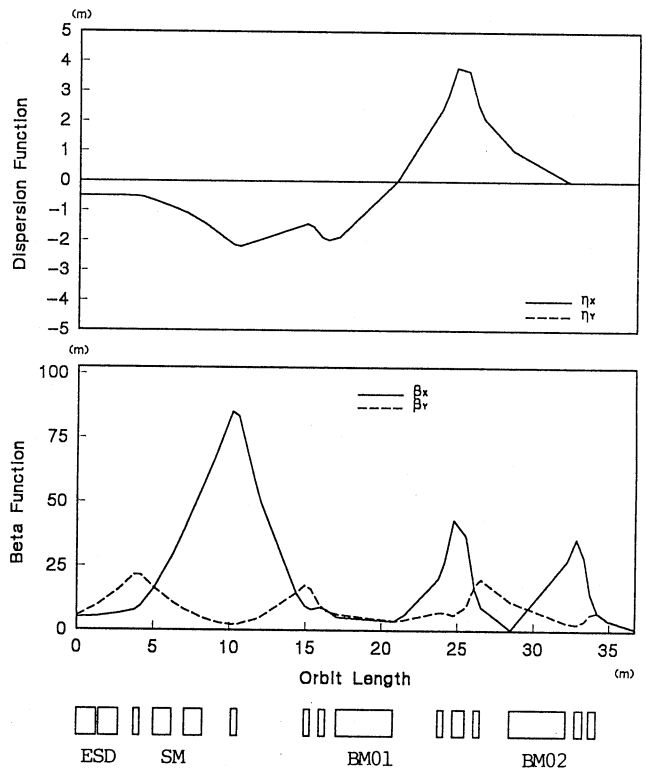


Fig. 4 Beta and dispersion functions in the extraction line.

Acknowledgment

The authors would like to express their gratitude to Dr. K. Kawachi and the members of the Division of Accelerator Research of NIRS for their supports and helpful discussions.

References

1. Y. Hirao et al., Proc of the 2nd European Particle Accelerator Conf., Nice, France, 280-282. 1990.
2. A. S. King et al., SLAC-183.
3. M. Kumada et al., Nucl. Instr. and Meth. 211(1983)283.
4. K. Kondo et al., Proc of the 7th Symp. on Accel. Sci. and Tech., Osaka, Japan, 149-151. 1989.
5. M. Torikoshi et al., These proceedings.
6. K. L. Brown, SLAC-75